An Assessment of Fission Fragments Enhancement for Nuclear Thermal Propulsion

Ivan Di Piazza*and Marco Mulas†

CRS4, Parco POLARIS, Pula (Ca) 09010, Italy

ABSTRACT

A novel concept of Nuclear Thermal Rocket (NTR) propulsion is presented. It is based on the direct conversion of the kinetic energy of the Fission Fragments (FFs) into the propellant enthalpy. The FFs can escape from an extremely thin layer of fissionable material: a sufficiently large surface coated with few micrometers of Americium 242m, confined by a neutron diffuser, may become a critical reactor. The novel FF NTR propulsion concept may allow the propellant to achieve temperatures higher than the nuclear fuel, thus overcoming the limit in the specific enthalpy achievable by the propellant in the conventional solid-core NTR propulsion. Such a limit comes from the need to keep the temperature of the fuel material within a safe interval by using conventional convective heat transfer mechanism. A preliminary assessment of the FF NTR concept's propulsion characteristics has been carried out using an in-house developed software system which integrates a Computational Fluid Dynamic code, a neutronic code and a Monte Carlo code. The assessment shows the potential to reach specific impulses of about 15,000 m/s and thrust levels in the range 4,000 to 6,000 N, with a trhust to weight ratio of a few percent of the acceleration of gravity. Such performances may make the FF propulsion a candidate for human missions to the planet Mars.

---

*researcher, group of Hydrology and Water Resources Management

†senior researcher, group of Computational Fluid Dynamics, member AIAA

1 Introduction

The NTR (Nuclear Thermal Rocket) represents a relatively mature advanced propulsion technology that can be considered for near future human missions to Mars [1, 2]. In principle, nuclear propulsion can allow much higher specific impulses, with respect to the use of chemical propulsion: the energy available from one unit mass of fissionable material is 10^7 times larger than that available from chemical reactions. The heat of combustion of the most energetic reaction (liquid oxygen and liquid hydrogen) limits the specific impulse (I_{sp}) to about 4 km/s[1], which corresponds to a specific enthalpy level of the propellant below 10^7 J/kg. Specific enthalpy levels of 10^8 and 10^9 J/kg, in principle easily attainable with the nuclear energy source, would lead to specific impulses well above 10 and 30 km/s respectively. By looking at the rocket equation 1, which limits the mission that any rocket can complete depending on the rocket specific impulse, such values may open the doors to interplanetary human space exploration:

$$M_p = M \left(e^{\Delta V / I_{SP}} - 1 \right) \tag{1}$$

where M_p is the mass of propellant needed to complete the mission, M is the total burnout mass (mass of spaceship at the end of the mission), and ΔV the velocity drop required by the mission. It is worth noticing that in the equation 1 the effects of gravity have been disregarded and so it is strictly valid for propulsion system with a high thrust to weight ratio.

NTR refers to conventional solid-core thermal rocket. It is based on conventional convective heat transfer mechanism between a solid "hot" material (fissioning fuel) and a "cold" propellant. Starting in the mid '50s, the NERVA (Nuclear Engine for Rocket Vehicle Application) NTR project [3] was developed in the US in order to make Mars exploration by humans feasible. In the NERVA concept the rods of a fission nuclear reactor were cooled by a hydrogen flow, with standard convective heat transfer mechanism. In order to keep the fuel rods temperature below safety limits, the engine was designed to run at very high mass flow rates of about $40 \ \text{kg/s}$ and at very high pressures in the order of 100 bar. The overall engine weight

---

[1]The specific impulse represents the thrust force exerted by the unit propellant mass flow rate and, in S.I. units, has the dimension of a velocity ([m/s]) and it is almost equal to the exhaust velocity of the propellant at the nozzle exit section. In old and historical units the specific impulse used to be measured as a force per unit propellant flow rate in weight, i.e. in seconds [s]. The ratio between the two numerical values is the acceleration of gravity $g = 9.81$.

was about 10 metric tons. A smaller version (with a mass flow rate of about 9 kg/s) was actually built and tested. When the program was terminated, ground tests showed the potential to reach specific impulses of about 9,000 m/s and thrusts of the order of 350 kN with the high mass flow rate version.

The specific impulse of a conventional NTR is thus clearly limited by the need to keep the structure temperature somewhere below 3,500 K, which corresponds to the hydrogen temperature in between 3,000 and 3,500 K. This means that NTR and chemical propulsion operate at the same propellant temperature of the order of 3,000/K, and that the superior performance of the NTR is therefore due only to the higher specific heat of the propellant (lighter molecular weight): hydrogen versus water vapor. As a result, propellant specific enthalpies are 5 times larger for an NTR with respect to the Space Shuttle case, and the gain in the specific impulse is little more than twice as much. Though this represents an important improvement, the energy delivered to the unit mass of propellant, and so the propellant temperature, is limited by the structure resistance and, in a sense, by the conventional heat transfer mechanism used to convey the energy from the nuclear source.

Recently developed technological variants of NTR, such as liquid oxygen (LOX) augmented NTR or bi-modal NTR-NEP (Nuclear Electric Propulsion) [4] do not change the potential of the baseline conventional solid-core NTR from a performance point of view.

Another concept of nuclear propulsion, based on fission reactions, is the so-called gas-core fission propulsion [5]. In such a device, the fissionable material is allowed to heat-up to plasma temperatures and its radiation is used to heat up the hydrogen gas. In this concept the propellant temperature can be significantly higher than the engine structural temperatures. The cooling of the engine walls remains however a major engineering problem [4]. This scheme can ideally reach specific impulses in the range of several tens of km/s, with a much larger weight (in the order of 100 metric tons) and a lower thrust in the range of 50 to 100 kN, and consequently a much lower thrust to weight ratio (T/W), compared to solid-core NTR. Such figures however would allow to shorten the total round trip time to Mars to less than a year [6], compared to over two and a half years needed to fly on the Hohmann route[2] [7]. However, the gas-core reactor represents a more far term option, for many technological challenges have still to be solved.

---

[2]The Hohmann transfer ellipse connects the orbits of Earth and Mars with minimum mission ΔV.

A new nuclear rocket concept has been recently introduced by Rubbia [8] and it is based on an idea also proposed by Chapline [9], Ronen [10] and Kammash [11], among others in the past two decades. Fission Fragments escaping an ultra thin layer of few micrometers of Americium 242m can be used to heat up a hydrogen flow. Heavy ionising fragments produced by neutron induced nuclear fissions carry the major part of the corresponding fission energy in the form of kinetic energy (about 168 MeV out of 191 MeV per fission). FFs convert all of their kinetic energy into internal energy of the propellant gas, slowing down via electromagnetic interaction, provided that a sufficient thickness of propellant is present (about 500 μg/cm^2 [8]). By this unconventional (direct) heat transfer mechanism, the enthalpy of the gas in the stagnation chamber can reach values of about $200 - 300$ MJ/kg, at low pressures of few bars, corresponding to temperatures of about 4,000 to $4,800$ K[3] and to a specific impulse I_{SP} of the order of $15,000 - 20,000$ m/s.

Compared to the convective heat transfer mechanism, the direct energy conversion may allow the propellant to heat up to temperatures higher than the material temperatures, thus outperforming the conventional NTR concept in terms of propellant specific enthalpies: the hydrogen flow may enter the stagnation chamber at low temperature (say in the range 1,500, 2,000 K) and can heat up, in principle without limits, flowing towards the nozzle.

The objective of the this paper is to present a preliminary assessment of the thermodynamic and propulsive performance of the unconventional, FF NTR. Advantages, disadvantages and open questions of the propulsion concept will be discussed, compared to the conventional NTR. Important scientific and technological aspects of the system, which are likely to play a very important role in the overall design process and would necessitate the interaction of many specialized scientific teams (neutronics outputs, physico-chemical behaviour of the Americium thin layer under thermal and mechanical stress, etc), are neglected or considered known, and some realistic assumptions are made. The scientific feasibility of the FF unconventional NTR concept has been demonstrated in [8], while in [12] an integrated software system developed and used for simulating the fluid dynamic and thermal behaviour of the system has been described.

---

[3]At such low pressures, compared to order 100 bar of conventional NTR, hydrogen dissociation occurs, with an associated enthalpy change of $\Delta h_{diss} = 230$ MJ/kg. This reaction contributes to store energy in the chemical bonds, rather than as sensible enthalpy, keeping the temperature lower.

The analysis have been performed on a single heating module with 3D axisymmetric simulations. The system is made of a CFD code coupled to a neutronic code and to a Monte Carlo code. The neutronic code was developed over the past two decades at CERN, the European Center of Particle Physics: for on a chosen fissile material and a given layer thickness, constructs a database containing the FF power density (in W/m^2), the percentage of FFs escaping the fuel layer and the kinetic energy distribution of the FFs [8]. The outputs of the neutronic code are then used by the Monte Carlo code for modelling the fission fragments emission from the fuel layer and the direct energy conversion into propellant enthalpy. An experimental validation of the interaction model is still not available. The CFD code, which computes the flow inside the engine, has been fully validated for a variety of compressible flows of fluids defined by arbitrary equations of state [13]: in this case the equation of state implements chemical equilibrium conditions for hydrogen, in a wide range of temperatures and pressures, by means of look-up tables obtained with the NASA CEA (Chemical Equilibrium for Application) code [14].

2 Engine description

2.1 General layout

The conceptual design is based on a number N of cylindrical modules (heating tubes) immersed in a bath of boiling Lithium at a temperature $T_{Li} \approx 2,000$ K. Figure 1 shows a schematic representation of the engine. The tubes are internally coated with an extra thin layer of ^{242m}Am: due to the high cross section of ^{242m}Am (one order of magnitude higher than that of ^{235}U), such a configuration represents a critical reactor confined by a neutron diffuser. Carbon (graphite) or Beryllium (Be or BeO) can be used as reflector-moderator around the engine, and a sort of n-hohlraum can be created, assuring a multiplication factor k_{eff} sufficiently high to give allowance of a reasonable Burn-up, even for a fissile layer of few micrometers of thickness. Hydrogen enters the tubes uniformly, permeating the solid walls, and heats up as it flows out of the heating tubes by stopping the FFs.

Figure 2 shows the so called Catiuscia arrangement of N heating tubes of diameter D. The tubes structure is made out of carbon composite fibers and matrices, a material which is porous and permeable
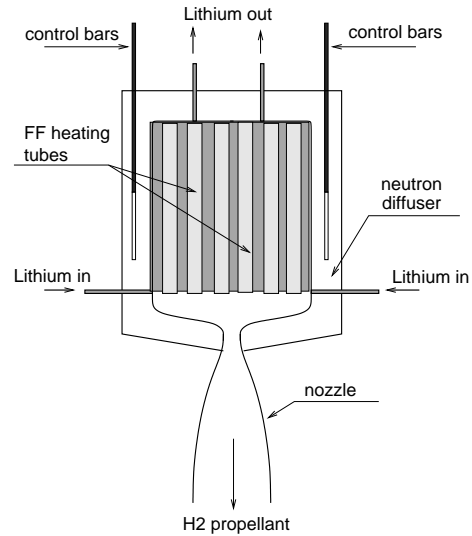
Figure 1: Schematic representation of the FF heated propulsion engine. The configuration is a critical reactor cooled by boiling Lithium and confined by a neutron diffuser. The heating chamber is made of a number of cilindrical tubes immersed in the Lithium bath. Though not shown in the Figure, hydrogen enters the system from the top of each heating tube as shown in the next Figure 2.

to hydrogen. A slab with thickness of the order of 1 to 2 centimeters with a limited number of narrow, hollow channels in which hydrogen can be introduced under pressure can provide the necessary mass flow rate of propellant $\dot{m}_p$. Preliminary simulations of the hydrogen flow through the porous material showed a pressure drop of about 40 atmospheres for a mass flow rate of about 4 g/s in a single heating tube. The simulations were carried out using a finite element model for the Darcy law with a porosity of 0.1 [15]. The computer model also included the evaluation of the structural stresses under the thermal and mechanical loads.

The thermo and fluid dynamic conditions of the propellant flowing inside the heating tubes depend on the volumetric heat addition coming from the FFs: the energy deposit, proportional to the local propellant density, heats up the propellant and so changes its temperature and density, modifying in turn the FF energy deposit itself. The final state of the propellant flow exiting the tubes, as well as the thermodynamic state in terms of temperature and pressure, comes from the equilibrium among many different effects: the conservation equations of mass, momentum and energy including a model for the FF heating ([8]) and the

H_2 dissociation. Once the fluid has been heated, it flows in the stagnation chamber, and then it is accelerated through a conventional convergent-divergent nozzle, where the internal energy is converted into kinetic energy generating thrust. The portion of nuclear fission energy which is not converted into propellant enthalpy must be evacuated by the lithium refrigerant that flows out of the core region through small tubes to the radiating panels. In a preliminary conception of the cooling system, the lithium would enter the system in liquid phase and would partially vaporise evacuating heat from the heating tubes. The lithium returns to the liquid phase flowing inside the radiative panels.
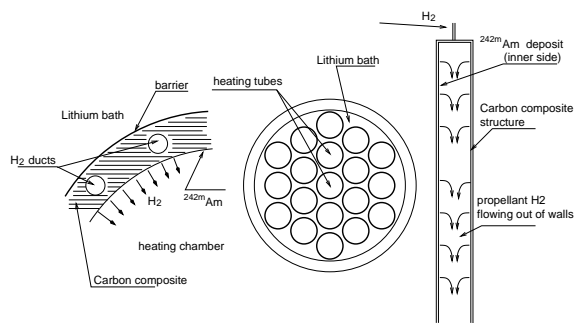

Figure 2: Cross section view of the heating chamber of the engine (*center*) with a schematic representation of the single tube (*right*): the cylinders are coated with the ^{242m}Am thin layer and cooled by the boiling Lithium; the H_2 propellant flow enters the cylinder uniformly from the tube walls. On the left: schematic representation of the permeable tube wall, based on the use of carbon composite fibers and matrices.

The number of modules which can be assembled together is limited by the size of the engine, which in turn is limited by the size of the Cargo bay of the next generation Space Shuttle, for the engine has to be assembled in the International Space Station and can only be ignited in space. The dimension of the actual Space Shuttle Cargo Bay are about 4.5 meters in diameter and 18 meters long. With the constraint of $D = 4$ m, three multiple-module arrangements are shown in Figure 3. The three configurations would fit 37, 19 and 7 modules, respectively with diameter 0.4, 0.6 and 1 meter. A perspective view of the assembled Catiuscia engine is shown in the Figure 4, where the length of the modules has been fixed to 5 meters.

The table 1 lists the numerical values assigned to a few variables (taken from the reference [8]) which play an important role in understanding the concept feasibility and in quantifying the engine performance. With regard to the physico-chemical form of the fuel layer, for instance, since metallic Americium melts at
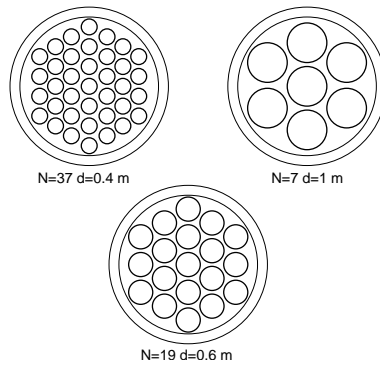
Figure 3: Three possible Catiuscia configurations with an external diameter of 4 meters. $N = 37, 19$ or 7 respectively for modules of diamater $D = 0.4, 0.6$ or 1.0 m.

Figure 4: Perspective view of the assembled Catiuscia engine. All modules discharge in the same nozzle.

1,270 K, Americium carbide represents a potential alternative. At this stage of the development however, the values listed refer to metallic Americium.

$B_{UP} = 500 \text{ MWday/kg}$	fuel Burn-up
$B_{UP} = 4.32 \times 10^{13} \text{ J/kg}$	fuel Burn-up (SI units)
$\delta_F = 3 \times 10^{-6} \text{ m}$	thickness of fuel layer
$\rho_F = 13,670 \text{ kg/m}^3$	density of fuel layer
$\dot{q}_{FF} = 4 \text{ MW/m}^2$	rate of fuel consumption

Table 1: Values of a few variables taken from reference [8]

2.2 Engine overall efficiency

The number of fissions that occurs in the engine per unit time and per unit surface of the fuel layer, determines the rate at which energy is transferred to the propellant, or the rate of fuel consumption $\dot{q}_{FF}$. The overall rocket engine efficiency η is defined as the ratio between the propulsion power $\dot{Q}_p$ and the gross nuclear power available from the fission process $\dot{Q}_F$:

$$\eta = \frac{\dot{Q}_p}{\dot{Q}_F} = \frac{\dot{m}_p \, V_{exit}^2/2}{N \, \pi D L \, \dot{q}_{FF}} \tag{2}$$

where $\pi D L$ is the available emission surface of a single heating tube, N is the number of heating tubes and $\dot{m}_p$ is the overall engine hydrogen mass flow rate. If h represents the average enthalpy level reached by the propellant mass flow rate $\dot{m}_p$ at the end of the heating process, and $\Delta h = h - h_w$ represents the enthalpy increase due to the heating process, with respect to a initial (wall) enthalpy level h_w, then the propulsion power can be computed as the heating stagnation power $\dot{Q}_h = \dot{m}_p \Delta h$ minus the nozzle losses:

$$\dot{Q}_p = \dot{Q}_h - \dot{Q}_{nozzle} = \eta_N \, \dot{Q}_h \tag{3}$$

where $\dot{Q}_{nozzle}$ represents the losses associated to the expansion process in the converging-diverging supersonic nozzle which are due to the missed chemical recombination into molecular hydrogen, and eventually to the frictional and heat flow losses at the nozzle walls. In the equation 3 the nozzle efficency $\eta_N < 1$ has been introduced. The gross fission fragment power $\dot{Q}_F$ is converted into heating stagnation power $\dot{Q}_h$ with several losses. This power budget can be expressed as:

$$\dot{Q}_h = \dot{Q}_F - \dot{Q}_{FF\_lost} - \dot{Q}_{cond} \tag{4}$$

where $\dot{Q}_{FF\_lost}$ represents the power associated to the fission fragments which remain entrapped in the fuel layer and in the tube structure or escape from the system, and never becomes available for heating the propellant; the third term, $\dot{Q}_{cond}$, on the righthandside represents the power loss due to heat conduction through the tubes walls. The Reynolds number associated to the flow inside the heating tubes may, in fact, be low enough so that heat conduction losses can be important. The two sources of power which are lost, return to the tube structure and need be evacuated by the Lithium refrigerant, through the radiative panels. By introducing two more efficiencies η_{FF}, which takes into account the FF losses, and η_h for the heat

transfer losses, then the heating power $\dot{Q}_h$, representing the power which remains availbale for conversion into propulsive power, is given by:

$$\dot{Q}_h = (\eta_{FF} \, \eta_h) \, \dot{Q}_F \tag{5}$$

or, by introducing $\eta_{FF} = \eta_{layer} \, \eta_{capture}$:

$$\dot{Q}_h = (\eta_{layer} \, \eta_{capture} \, \eta_h) \, \dot{Q}_F \tag{6}$$

where the FF losses have been split into two contributions: one, η_{layer}, due to the FFs which leave part or all of their power inside the fuel layer (FFs that cannot escape from the thin layer, for instance), and the second one, $\eta_{capture}$ due to insufficient gas thickness present inside the tube to stop all available FFs escaping from the fuel layer. By combining all relations, an expression for the overall engine efficiency η is given by:

$$\dot{Q}_p = (\eta_{layer} \, \eta_{capture} \, \eta_h \, \eta_N) \, \dot{Q}_F = \eta \, \dot{Q}_F \tag{7}$$

Now, η_{layer} depends on the fuel thickness (the thinner the layer, the higher η_{layer}), on the fuel chemical form (metallic rather than carbide, for instance) as well as on neutronic issues, and it is always less than 0.5 for symmetry reasons (half of the FFs would tend to escape from the wrong side, converting their energy into heat of the wall structure). In this work, a layer of metallic ^{242m}Am of thickness $\delta_F = 3 \times 10^{-6}$ m and density $\rho_F = 13,670$ kg/m^3 has been assumed. Neutronic simulations based on these figures provided a value for the layer efficiency given by $\eta_{layer} = 0.31$ [8], which means that 70% of the overall power $\dot{Q}_F$ is instantaneously converted into heat.

The second efficiency $\eta_{capture}$ measures the amount of power extracted by the FFs during the interaction with the flowing propellant and depends upon the gas thickness and on the propellant thermodynamic pressure as a consequence. Its actual value depends on the design choices in terms of operating pressure and nozzle throat area: the highest the pressure, the highest $\eta_{capture}$ (eventually approaching unity), but the tightest the throat area and (eventually) the highest the nozzle losses (heat transfer losses). Values obtained in the simulations carried out, are in the range between 0.75 and 0.95.

FFs that remain entrapped into the structure may determine material damage and structural swelling due to further FF decay. These issues have not been studied and may need further investigations.

The third efficiency, called the heating efficiency, measures the power loss due to the heat conduction through the tube walls. The heating efficiency is the crucial efficiency, for it can vary widely in between 0 and 1, depending on the operating conditions. High mass flow rates (high Reynolds numbers) will allow a high η_h, a low propellant specific enthalpy and a low specific impulse. On the contrary, high specific impulses and low efficiencies will be obtained running the engine at low mass flow rates, due to increased conductive losses.

Finally η_N is the nozzle efficiency. The value of $\eta_N \approx 0.60$ represents a good approximation if the accelerating flow inside the nozzle remains in chemical equilibrium conditions, and if negligible viscous and wall heat transfer losses occur. This will turn out to be a good approximation if the nozzle dimensions are not too small (again, a high nozzle Reynolds number contributes to disregard heat transfer losses: the nozzle throat area does not have to be too small). Again, the design pressure in the stagnation modules appears as one of the critical design choices for the whole system. The lower possible pressure seems to be the optimal choice, provided that $\eta_{capture}$ remains at an acceptable level.

η_{layer}	0.3	depends on fuel layer (< 0.5)
$\eta_{capture}$	0.75-0.95	depends on propellant pressure
η_h	0 - 1	depends on tube Reynolds number
η_N	0.6	depends on nozzle Reynolds number
η	$< 0.14 - 0.17$	$\eta = \eta_{layer}\, \eta_{capture}\, \eta_h\, \eta_N$

Table 2: Summary of all partial efficiencies of the FF NTR concept. The second column shows the numerical values used in this work.

A summary of all efficiencies is given in the table 2 for the sake of clarity. By considering the values discussed above, then the overall engine efficiency η is smaller than about 0.16. The power losses associated to ($\eta_{layer}\, \eta_{capture}\, \eta_h$) represent the heat that must be removed by cooling the external walls by the Lithium loop, and by the radiative panels. If $\eta_h \approx 1$ such a power loss amounts to the 74% (minimum) of the gross nuclear power. The remaining 10% of the initial power is associated to the nozzle efficiency and represents mostly the power stored in the chemical bonds of atomic hydrogen (missed recombination of molecular hydrogen in chemical equilibrium conditions). This portion is is directly lost towards the deep space. The

lower η_h, with respect to unity, the higher the power percentage that must be evacuated through the Lithium loop, which must then be designed for evacuating the whole power, as in the case of zero propellant mass flow rate with the nuclear reactor operating at 100% power.

In the next section a correlation for the heating efficiency η_h is given, based on 1D approximation.

3 An approximate analytical model of the single module

3.1 The 1D approximation

The model is based on the mass and power balances of the single heating module of diameter D and length L, schematically shown in Figure 5.
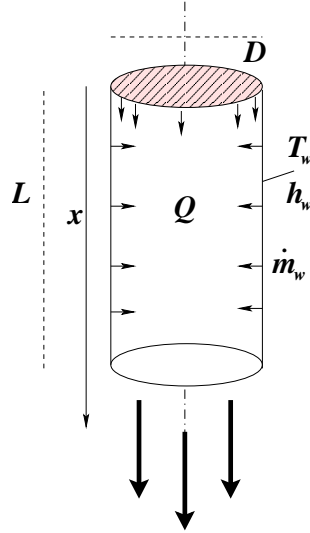

Figure 5: Schematic representation of the heating module.

The walls are kept at a constant temperature T_w, and thus the propellant will be pre-heated while permeating the solid walls of the carbon-carbon structure, and it will enter the heating tube with the inlet enthalpy h_w. The heating process by the FFs can be approximately described by a constant power per unit volume $\dot{Q}$ (units W/m^3), given by:

$$\dot{Q} = \frac{\dot{q}_{FF}\, \eta_{FF}\, \pi DL}{\pi D^2/4\; L} \tag{8}$$

The mass flow rate is provided from the solid wall at a constant specific rate per unit area $\dot{m}_w$ (units

kg/m^{2}s). If an x coordinate system is defined along the module axis, mass and energy balances can be made with reference to an infinitesimal portion dx of the module of volume $dV = \pi \frac{D^2}{4} dx$. The theory will be illustrated in a concice way, while for detailed explanation the reader can refer to the report [16]. The balances refer to sections located far from the top of the module, in which an asymptotyc radial temperature profile, and thus an asymptotic section-average enthalpy level have been reached.

It can be shown that the mass flow rate at the exit section located at L is:

$$\dot{m}(L) \approx \dot{m}_w \, \pi D L \tag{9}$$

The energy balance can be written in the following way:

$$dQ_{gen} = dQ_{conv} + dQ_w \tag{10}$$

where dQ_{gen} is the power deposited in the volume dV, while dQ_{conv} and dQ_w represent the power extracted by convection and the power loss for heat conduction at the walls. The three pieces of equation 10 can now be estimated separately. The power generation in the volume dV is:

$$dQ_{gen} = \dot{Q} \, \pi \frac{D^2}{4} \, dx \tag{11}$$

If $h(x)$ is the average gas enthalpy at section x, and by introducing the new variable $\Delta h(x) = h(x) - h_w$, the power extracted by convection in the volume dV can be computed as:

$$dQ_{conv} \approx \Delta h(x) \, \dot{m}_w \pi D \, dx \tag{12}$$

For relatively low Reynolds numbers and with internal heat generation the temperature profile maintains the parabolic shape of the pure conductive case. The wall heat flux q''_w can then be expressed as:

$$q''_w = f \, \frac{16}{3} \frac{k \, \Delta h}{c_p D} \tag{13}$$

where a correction factor $f > 1$ has been introduced to account for the higher FF power deposition close to the walls due to the hydrogen higher density. The CFD calculations showed that a correction factor $f \approx 1.5$ is appropriate.

From this relation, the total power exiting from the side walls in the volume dV can then be written as:

$$dQ_w = q''_w \pi D \, dx = \frac{16}{3} f \, \pi \frac{k}{c_p} \, \Delta h \, dx \tag{14}$$

With the terms 11, 12 and 14 explicitly written, the power balance 10 can be revisited. The enthalpy drop can thus be finally expressed as:

$$\Delta h = \frac{\dot{Q}D^2/4}{\dot{m}_w D + \frac{16}{3} f \frac{k}{c_p}} \tag{15}$$

3.2 A correlation for the heating efficiency

The heating efficiency η_h can be derived from the main result of the analytical 1-D model 15. In fact, the heating efficiency is defined as:

$$\eta_h = \frac{\dot{m}(L)\Delta h}{\pi D L \, \eta_{FF} \dot{q}_{FF}} \tag{16}$$

By introducing the expressions derived for $\dot{m}(L)$, Δh and $\dot{Q}$ in equation 16, it is possible to express the heating efficiency in the following way:

$$\eta_h = \frac{Pe}{1 + Pe} \tag{17}$$

where Pe is the tube Peclet number defined as:

$$Pe = \frac{3}{16} \frac{1}{\rho \, \alpha \, f} \dot{m}_w D \tag{18}$$

where α represents the thermal diffusivity (units m^2/s). The Peclet number represents the product of the Prandtl number $Pr = \nu/\alpha$ (ν is the kinematic viscosity) and a particular form of a Reynolds number given by:

$$Re = \frac{3}{16} \frac{1}{\rho \, \nu \, f} \dot{m}_w D \tag{19}$$

where all the physical properties are to be evaluated at a constant average temperature. A comparison between the correlation 17 and the heating efficiencies computed with CFD calculations is shown in Figure 6: an excellent agreement is found.
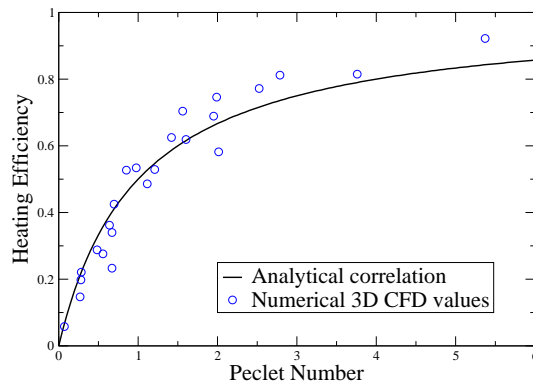
Figure 6: Comparison between analytical correlation for heating efficiency and three-dimensional numerical simulations.

4   Performance assessment

4.1   FF engine optimization

The requirement of a rocket engine is to accomplish a given interplanetary mission. This implies to choose a target planet, say Mars, and the route to get to it, so that the mission ΔV can be determined. The cheapest way to get to Mars is on the Hohmann transfer. A round trip from the low Earth orbit (LEO) of the International Space Station to a low Mars orbit (LMO) would require a velocity change of about $\Delta V = 23,000$ m/s. If, in 20 or 30 years from now, humans will routinely travel to Mars, it is reasonable to think of starting from an LEO co-planar to the ecliptic: moving the ISS orbit from today's 51° to 23°, will reduce the overall velocity change from LEO to LMO and back, on a Hohmann transfer, to about $\Delta V = 11,500$ m/s.

For the sake of simplicity, and to fix ideas, without entering into the mission design business, one may think of mission requirements of, for instance, 12 and 6 km/s: the first one can represent either a round trip requirement on a Hohmann transfer, or a one way trip on a faster route (inbound or outbound); the second one may represent a one way trip on a Hohmann transfer. The idea could be of having light spaceships, with crew onboard, running on faster than Hohmann transfers and using FF propulsion. On the other hand, one way unmanned heavy cargo missions on Hohmann transfer can be devised to bring all that would be needed to land on the planet, to stay the required time and also to bring the return spaceship for the crew to

get back to the Earth. For such cargos, different propulsion systems would be used. What matters are the manned trips which should move the crew quickly and safely.

One important concern is about availability of the nuclear fuel: there must be enough nuclear fuel M_F for accomplishing the mission. In other words the nuclear reactor must be able to keep criticality at the full nominal power for a time lag at least equal to the time needed to consume all the propellant at the nominal mass flow rate.

The time τ_F needed to exhaust all nuclear fuel is given by the ratio of the engine gross energy E_F to the engine gross power $\dot{Q}_F$:

$$E_F = M_F B_{UP} = N S \delta_{Am} \rho_{Am} B_{UP} \tag{20}$$

$$\dot{Q}_F = N S \dot{q}_{FF} \tag{21}$$

where S is the available emission surface of a single module, N the number of modules, B_{UP} is the fuel Burn-up (a sort of percentage of nuclear fuel available to run the reactor before falling short of criticality), and $\dot{q}_{FF}$ represents the rate at which the nuclear fuel is burnt (expressed in W/m^2, related to the number of FFs escaping the fuel layer in the unit time and from the unit surface area). Since both terms scale with the total surface area NS, τ_F does not depend on the number of modules, nor on their diameter.

$$\tau_F = \frac{E_F}{\dot{Q}_F} = \frac{\delta_{Am} \rho_{Am} B_{UP}}{\dot{q}_{FF}} \tag{22}$$

The time τ_F represents then the engine maximum duration, depends only on the layer thickness and on neutronic and nuclear criticality issues, and it is inversely proportional to of the rate of fuel consumption.

On the other hand, the time τ_P needed to consume all the propellant mass M_P, is simply given by the ratio of M_P to the propellant mass flow rate $\dot{m}_p$. By using the rocket equation 1:

$$\tau_P = \frac{M_p}{\dot{m}_p} = \frac{M \left(e^{\Delta V / I_{SP}} - 1 \right)}{\dot{m}_p} \tag{23}$$

Without resorting to refueling options, the mission is possible if the engine maximum duration τ_F is greater than the propellant time τ_P:

$$\tau_F > \tau_P \tag{24}$$

or

$$\Delta V < I_{SP}\, ln\left(\frac{\dot{m}_p\, \tau_F}{M} + 1\right) \equiv \Delta V_{limit} \tag{25}$$

which means that the achieveble ΔV may be limited by fuel shortage rather than by weight or propellant

issues, though re-fueling may represent a technical option.

D	N	M_F	$\dot{Q}_F$	$\dot{q}_{FF}$	τ_F	L
m	-	kg	MW	MW/m^2	$days$	m
0.4	37	4.8	230	2	8	2.5
0.6	19	3.7	179	2	8	2.5
1.0	7	2.3	110	2	8	2.5
1.0	7	2.3	220	4	4	2.5
1.0	7	4.6	220	2	8	5.0
1.0	7	9.2	440	4	4	5.0

Table 3: Examples of engine configurations and corresponding overall engine power

The table 3 shows the engine overall power, fuel mass and time of fuel duration τ_F, for various engine

configurations in terms of number of modules and their diameter, length of the modules and the rate of fuel

consumption $\dot{q}_{FF}$.

The Figure 7 shows a schematic representation of the optimization process: starting from the mission

requirements, a number of design choices have to be optimized in order to make the mission possible. The

number of modules, their diameter, the overall propellant mass flow rate and the type and quantity of the

nuclear fuel determine the engine overall efficiency, the specific impulse and the fuel Burn-up such that

there will be enough fuel and enough propellant to complete the mission. Engine power, weight and thrust

also represent results of the optimization procedure.

Running the engine at low efficiencies may determine the danger of running out of nuclear fuel. On

the oher hand, the overall efficiency can be increased paying a price in terms of lower specific impulse. In

other words the trade-off is between higher efficiency and higher specific impulse. The pressure that is to

be established inside the heating tubes has an influence on the $\eta_{capture}$ (the higher the pressure, the better
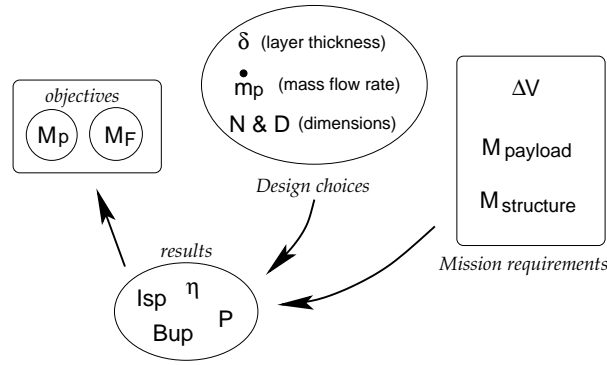
Figure 7: Schematic representation of the optimization process for the FF rocket engine

the efficiency), and also on the throat area and on the nozzle efficiency as a consequence (the lower the pressure, the larger the nozzle and its Reynolds number, and so the higher η_N and the overall efficiency).

The criticality of the system has also to be ensured. The references [17] discuss this issue: clearly the reactor multiplication factor k_{eff} increases by increasing the overall fuel mass M_F, using more modules of smaller diameter, with a higher operating pressure in order to keep $\eta_{capture}$ high. The engine must provide a sufficiently high reactivity reserve to accomplish the mission. In other words, the Burn-up must be as higher as possible. A higher Burn-up may be obtained increasing the thickness of the fuel layer, which in turn decreases η_{layer} together with the overall engine efficiency. The engine weight depends on the surface area of the radiative panels, which scales with the engine power, and on the size (weight) of the neutron diffuser, which depends on the multiplication factor k_{eff}. Last but not least, the engine length (the length of the modules) has an influence on the overal power and on the k_{eff}.

So, an engine configuration with many small tubes needs a higher pressure and may determine a lower efficiency (though however increases the k_{eff} and the Burn-up). The reverse is true for an engine configuration made of few large tubes. A global engine optimization is a problem whose solution is beyond the objectives of the present preliminary performance assessment. The understanding of how the optimization problem has to be set, will however provide the guidelines for a preliminary parametric analysis of the engine performance.

4.2 Results and discussion

A parametric analysis of the engine performance has been carried out. The analysis have been performed on a single heating module with 3D axisymmetric simulations using a hybrid integrated software system described in [12] which integrates a CFD code and a Monte Carlo code. The latter code models the FFs trajectories into the hydrogen flow and the direct energy conversion. The focus of the analysis was on the simulation of the heating process, without considering the supersonic expansion in the converging-diverging nozzle. Input to the system are a database containing the FF power density (in W/m^2), the percentage of FFs escaping the fuel layer and the kinetic energy distribution of the FFs.

The results can be expressed in terms of pressure and temperature fields, average enthalpy level of the propellant h, and efficiencies η_{layer}, $\eta_{capture}$, η_h. The nozzle efficiency η_N has been estimated with the NASA open source code CEA [14], and a value of $\eta_N = 0.60$ has been assumed in the study. 3D complete simulations of the whole engine [18] have shown the basic consistency of this assumption. Once the nozzle efficiency is known, the specific impulse I_{SP} can be easily derived from the enthalpy h of the gas in the stagnation chamber. Each engine configuration listed in the table 3 has been calculated for three different mass flow rates [4].
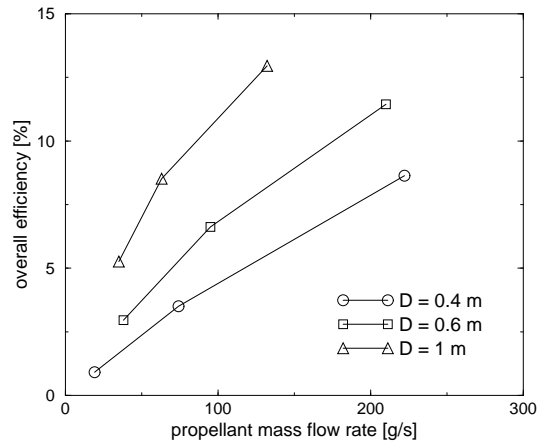
Figure 8: Overall efficiency versus the engine mass flow rate.

---

[4]It can be shown via nondimensional scale analysis that in the proximity of the planets, buoyant forces are negligible with respect to inertial forces, and thus buoyancy has not been considered in the numerical simulations. During the trip, in microgravity conditions, buoyant forces are absent. On the other hand, the maximum acceleration is limited by the system's thrust to weight ratio which is, as it will seen later on in this paragraph, only a few percent of g_0, the acceleration of gravity at the Earth surface.
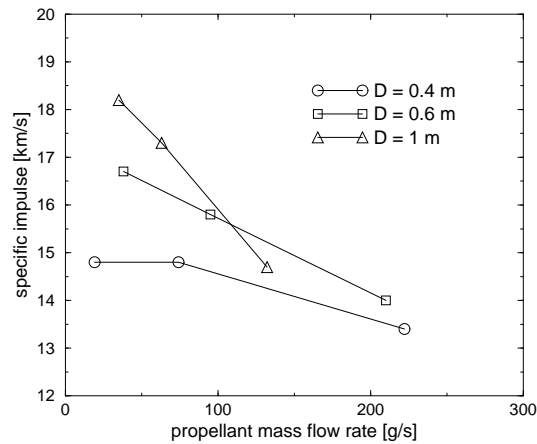
Figure 9: Specific impulse versus the engine mass flow rate.

The Figures 8 and 9 show the results in terms of overall efficiency and specific impulse respectively versus the engine mass flow rate. For all configurations, at the low mass flow rate regime the specific impulse is maximum and the efficiency minimum. At the high mass flow rate regime there is the tendency to approach the maximum possible overall engine efficiency of about 15-16% (zero conductive losses at high tube Reynolds numbers, and $\eta_h = 1$). The quantitative results are shown in the table 4. All results refer to 2.5-meter long modules, and to a rate of fuel consumption of $2 \ \mathrm{MW/m^2}$, but the last group which has double rate of consumption. The last column shows the attainable velocity change before exhausting the fuel, for a total mass of the spaceship at the end of the mission of of 50 metric tons. The mission velocity drop has been calculated using the simplified version of the rocket equation which disregard the gravity terms. A higher effective mission velocity drop has to be considered for propulsion system with low thrust to weight ratio.

As shown in the previous table 3, doubling the rate of fuel consumption $\dot{q}_{FF}$, for the 1-meter diameter configuration, results in doubling the overall engine gross power from 110 to 220 MW, and in halving the time of fuel duration τ_F, which has an influence on the maximum velocity change achievable (the engine runs out of fuel in half of the time). However, the overall efficiency improves.

Note that the limit in the achieveble velocity change refers to exhausting the fissile fuel, and does not have anything to do with exhausting the propellant. By finding efficient and reliable engineering solutions to re-fueling, the ΔV limit would be eliminated. Nevertheless, many of the achievable velocity changes listed

D	$\dot{m}$	η	I_{sp}	$\mathcal{T}$	ΔV
m	g/s	$\%$	m/s	N	km/s
0.4	19	0.91	14800	280	3.5
0.4	74	3,51	14800	1100	10.7
0.4	222	8.63	13400	3000	19.2
0.6	38	2.96	16700	640	7.3
0.6	95	6.62	15800	1500	13.6
0.6	210	11.44	14000	2950	19.5
1.0	35	5.26	18200	640	7.4
1.0	63	8.52	17300	1100	11.1
1.0	132	12.95	14700	1950	15.6
1.0	105	8.72	19100	2000	10.7
1.0	197	13.17	17100	3400	15.1
1.0	280	15.32	15500	4300	17.1

Table 4: Summary of performance of FF unconventional NTR propulsion. The last column shows the limit ΔV that can be accomplished for a burnout mass (final mass) $M = 50$ metric tons.

in the table are well above 12 km/s, which was taken as a reference value for representing a requirement for a one-way trip on a faster-than-Hohmann transfer route.

It is worth noticing that the slow reaction configuration with 37 modules and 40 cm diameter is equivalent, from gross power point of view, to the fast reaction configuration with 7 modules and 100 cm diameter. Doubling the module length, to 5 meters, also would result in doubling the gross power, in this case however paying a price in terms of a heavier spaceship, but with the same time τ_F. A 5-meter long version with the fast rate of consumption (4 MW/m^2), for the 7-tube and $D = 1$ m arrangement, and a mass flow rate of the order 600 g/s, would have a gross power of 440 MW, a specific impulse above 15,000 m/s and a thrust in the vicinity of 10,000 N.

Operating pressures for the three diameter choices are in the range 1.5 to 3 bars, for the larger and smaller diameters respectively. Average propellant stagnation temperatures, before expansion in the super-

sonic nozzle, would be in the range 4,000 to 4,800 K, respectively for specific impulses in the range 15,000 to 18,000 m/s, and would depend also on the operating pressure (the lower the pressure, the higher the dissociation level and the lower the average temperature). These figures are based on the CEA code [14].

In addition, while the diameter D diminishes, the neutronic efficiency of the system increases, and thus the reactivity reserve (i.e. the Burn-up) to accomplish the mission increases. Because there exist a technological Burn-up limit of about 30%, with respect to this feature, the best diameter would probably be the one that garantees this technological Burn-up. From the point of view of the residual power to bring out of the system, a fixed reactivity reserve can be reached much more efficiently with smaller diameters. Concerning the weight of the spaceship, the larger the diameters of the heating tubes, the larger the moderator (Beryllium) structural mass, due to the lower multiplication factor k_{eff}. Preliminary estimations indicate that the Beryllium mass can grow from 20 to 60 tons switching from the 60-cm to the 100-cm tube configuration. From these considerations, it appears that, from a neutronic point of view, small diameters would be favoured, which seems in contrast with the results of the table 4. Finally, preliminary design of the Lithium cooling system shows that two "sails" of approximately 13×6 m^2 would be needed to evacuate 100 MW power, with an overall mass smaller than 1 ton. These figures show an approximate thrust to weight ratio of the FF nuclear propulsion system similar to that of the Gas-core nuclear reactor: a few percent of g_0, where g_0 represents the acceleration of gravity at the Earth surface. As for the conventional NTR, a liquid oxygen augmentation would represent a potential system for increasing the thrust, at the expenses of decreasing the specific impulse. All these comments call for additional detailed studies leading to an accurate optimization process that take all variables into account.

5 Conclusions

The novel concept of unconventional NTR propulsion has been described and discussed. As opposed to conventional solid-core NTR propulsion, which relies on the convective heat transfer mechanism to convey the energy from the nuclear source to the propellant, the unconventional NTR is based on the direct conversion of the Fission Fragments kinetic energy into propellant enthalpy.

A preliminary assessment of the propulsion characteristics has been discussed. The potential to reach

specific impulses above 15,000 m/s has been shown. Though based only on theoretical assumptions and on computer simulation, this result represents an important improvement with respect to conventional NTR specific impulse of about 9,000 m/s.

The FF rocket concept can have operating conditions, in terms of mass flow rate, thrust and specific impulse, modulated depending on the mission requirements. Another difference with the case of chemical and conventional NTR propulsion, is that the achievable velocity change may be limited due to fuel shortage rather than to propellant shortage.

The main disadvantages, with respect to conventional NTR, are the low overall efficiency, below 16%, the lower thrust to weight ratio due to the mass of the neutron diffuser and the larger size, due to the radiative panels.

A number of key issues must still be investigated with wind tunnel experiments and more and extensive computer simulation. The chemical form of the fuel has to be devised, and the physico-chemical behaviour of the fuel layer has to be studied and tested under realistic conditions in a nuclear reactor. More studies and experiments must be devoted for assessing the effective nozzle efficiency, which was assumed equal to 0.6 throughout the paper. A further decrease of the nozzle efficiency, due to wall heat flux, may put the whole concept in jeopardy.

Finally, finding engineering solutions for re-fueling during the mission would represent a major step ahead for demonstating the feasibility of the novel rocket propulsion concept for allowing human missions to the planet Mars.

Acknowledgements

References

[1] L.T. De Luca editor, Proceedings of "The tenth international workshop on combustion and propulsion: In-Space Propulsion", Lerici, Italy 21-25 September 2003.

[2] *Nuclear propulsion and power for space: a roundtable discussion*, in Aerospace America, November 2004, pp.26-39.

[3] *Nuclear thermal rockets: next step to space*, in Aerospace America, June 1989, pp.16-29.

[4] R.H. Frisbee, *Advanced Space Propulsion for the 21st Century*, J. Propulsion and Power, vol.19, no.6, 2003, pp.1129-1154.

[5] J.D. Clement and J.R. Williams, *Gas core reactor technology*, Reactor Technol. 13, 3, 1970.

[6] S.D. Howe, B. DeVolder, L. Thode and D. Zerkle, *Reducing the risk to Mars: the gas-core nuclear rocket*, Proceedings of the Space Technology and Applications International Forum (STAIF), Los Alamos, Rept. LAUR-97-3361.

[7] *Special report: sending astronauts to Mars*, in Scientific American, March 2000.

[8] C. Rubbia, *Fission fragments heating for space propulsion*, CERN SL-Note 2000-036 EET, 2000.

[9] G. Chapline, *Fission fragment rocket concept*, Nucl. Instr. and Meth. A 271, pagg. 207-208, 1988.

[10] Y. Ronen and E. Shwageraus, *Ultra thin ^{242m}Am fuel elements in nuclear reactors*, Nucl. Instr. and Meth. A 455, pagg. 442-451, 2000.

[11] T. Kammash et al, *An Americium-fueled gas core nuclear reactor*, AIP Conference Proceedings, vol. 271(1), pag. 585, 1993.

[12] M. Mulas, I. Di Piazza, P. Pili, A. Varone, *Simulation of high enthalpy flows directly heated by the kinetic energy of fission fragments*, CRS4 report, 2002.

[13] M. Mulas, S. Chibbaro, G. Delussu, I. Di Piazza, M. Talice, *Efficient parallel computations of flows of arbitrary fluid for all regimes of Reynolds, Mach and Grashof numbers*, Int. J. of Num. Meth. for Heat & Fluid Flow, vol.12, no.6 (2002)

[14] B.J. McBride, S. Gordon: *Computer Program for Calculating and Fitting Thermodynamic Functions*, NASA RP-1271, 1992.

[15] L. Massidda and G. Fotia: *Progetto 242: sviluppo di un modello numerico per il calcolo della struttura*, CRS4 report, 2000.

[16] I. Di Piazza, *An analytical Model of Heat Transfer and Fluid Dynamic Performances of an Unconventional NTR Engine for Manned Interplanetary Missions*, CRS4 report, 2004.

[17] P. Benetti, L. Cinotti, M. Mulas and R. Stalio, *Fission fragments direct heating of gas propellant for space rocket*, in the proceedings of "The tenth international workshop on combustion and propulsion: In-Space Propulsion", Lerici, Italy 21-25 September 2003.

[18] I. Di Piazza, M. Mulas, A. Varone *Thermo-Fluid Dynamic Analysis of the Fision Fragments Rocket Engine*, Proceedings of UIT Conference, Trieste, Italy, June 2003.